EARTHQUAKE ENGINEERING AND STRUCTURAL DYNAMICS
Earthquake Engng. Struct. Dyn. **27**, 487–502 (1998)

POUNDING OF SUPERSTRUCTURE SEGMENTS IN ISOLATED ELEVATED BRIDGE DURING EARTHQUAKES

ROBERT JANKOWSKI,* KRZYSZTOF WILDE AND YOZO FUJINO
Department of Civil Engineering, University of Tokyo, Hongo 7-3-1, Bunkyo-ku, Tokyo 113, Japan

SUMMARY

Past severe earthquakes indicate that pounding may cause considerable damage or even lead to collapse of colliding structures. The aim of this paper is to present an analysis of pounding between superstructure segments of an isolated elevated bridge induced by the propagating seismic wave. High-damping rubber bearings (HDRBs), used as isolation devices, are modelled by proposed non-linear formulation and the significance of the bearings model for pounding is indicated. The results of the study show that pounding leads to the increase or decrease of the forces acting on piers, depending on the gap size between superstructure segments. © 1998 John Wiley & Sons, Ltd.

KEY WORDS: pounding; elevated bridge; earthquake excitation; high damping rubber bearing

INTRODUCTION

The surveys on damage during past severe earthquakes show that pounding can lead to considerable damage or even collapse of buildings if the separation distance between them is not sufficient.[1–3] Similarly in bridges, collisions may occur between an abutment and girder, adjacent girders or a girder and neighbouring structure due to their different phase vibrations. In the Loma Prieta earthquake (1989), pounding of the lower roadway and columns supporting an upper-level deck of the Southern viaduct section at the China Basin[4] (California) led to significant damage to the decks and columns' sides. The different heights, and therefore, the difference of natural frequencies of neighbouring bridge members was identified as the cause of collisions.[4] The influence of pounding of superstructure segments, supported on piers of equal height, on the structural response was confirmed on a highway bridge located 85 km away from Los Angeles.[5] The bridge was instrumented with a set of accelerometers and the collected records showed spikes, in some cases, of magnitude 10 times higher than the maximum acceleration of the earthquake input. The presence of spikes in the bridge response was explained by collisions induced by the seismic wave propagation effect.[5] The reports of damage to highway bridges during the Kobe earthquake (1995) also identify pounding due to fracture of bearing supports as a reason for local damage and a potential contribution of falling down of bridge decks (for example, Reference 6). Generally speaking, the forces induced by pounding of bridge components can be very large, resulting in significant additional loading transmitted to the lower part of the bridge. Moreover, the impact character of pounding forces increases the possibility of brittle fracture of structural members.

Most of the research work done so far has been focused on pounding of inadequately separated buildings with different dynamic characteristics. The fundamental study using single-degree-of-freedom models of buildings was carried out by Anagnostopoulos.[7] His results show that collisions usually amplify the structural response. More detailed analyses were conducted on multi-degree-of-freedom lumped mass

* Correspondence to: Robert Jankowski, Division of Structural Mechanics, Department of Civil Engineering, Technical University of Gdańsk, ul. Narutowicza 11/12, 80-952 Gdańsk, Poland

CCC 0098–8847/98/050487–16$17·50

Received 5 June 1997
Revised 1 September 1997

systems in which contact points were *a priori* determined.[8–10] Papadrakakis extended the study on pounding of buildings using FEM to also capture contacts in unknown locations.[11]

The most natural way to prevent pounding of buildings is to provide sufficiently large spacing between adjacent structures. The minimum seismic gap is specified in several earthquake resistant design codes.[12] To enhance the seismic performance of existing buildings without sufficient space between, a number of pounding mitigation techniques have been proposed. Westermo[13] suggested linking structures by beams which can transmit the forces between buildings, thus, completely eliminating dynamic contacts. The connections between adjacent structures can also have energy dissipating properties[14] and the blows of pounding can be partly absorbed. The idea of providing strong collision walls protecting the rest of building has been analysed by Anagnostopoulos.[15]

In contrast to buildings, the problems of pounding in bridges have not been studied much. Few results are available from the analysis of dynamic contacts between superstructure and abutment in short single-span bridges. Ma and Pantelides[16] carried out an analysis of bridge-abutment collisions using a single-degree-of-freedom inelastic model. Kawashima and Yabe[17] analysed different unseating prevention and energy dissipation devices to suppress the bridge response in order to minimize pounding with the abutment.

The use of seismic isolation in bridges, which became popular particularly in Japan after the Kobe earthquake, elongates the natural period of the structure, resulting in large displacements which increase the possibility of pounding. The earthquake design codes[18] specify that the gap size between bridge segments should be large enough to avoid collisions. On the other hand, however, enlarging the expansion joints between girders is expensive and an undesirable solution.

The purpose of this paper is to analyse pounding of adjacent superstructure segments of isolated elevated bridge induced by the seismic wave propagation effect. The first part of the paper presents a mathematical model of the bridge, including pounding and non-linear formulation of high-damping rubber bearings. In the second part, a response analysis under several earthquake records is conducted and the optimum gap size between superstructure segments is discussed.

MODELLING OF POUNDING IN ISOLATED ELEVATED BRIDGE

The effective isolation of superstructures in elevated bridges requires flexible bearings and very stiff piers. In such bridges,[19] the ratio between the natural frequencies of the pier-dominant mode and deck-dominant mode is usually bigger than 10. Thus, the contribution of the dynamics of piers to the total response of the structure is relatively small and may be neglected in a study of the fundamental aspects of pounding. Under this simplification, every superstructure segment can be treated as a one-degree-of-freedom system with lumped mass M_i mounted on spring-dashpot element which combines parameters of all bearings supporting the segment, $K_i = \sum K_b$, $C_i = \sum C_b$ (Figure 1).

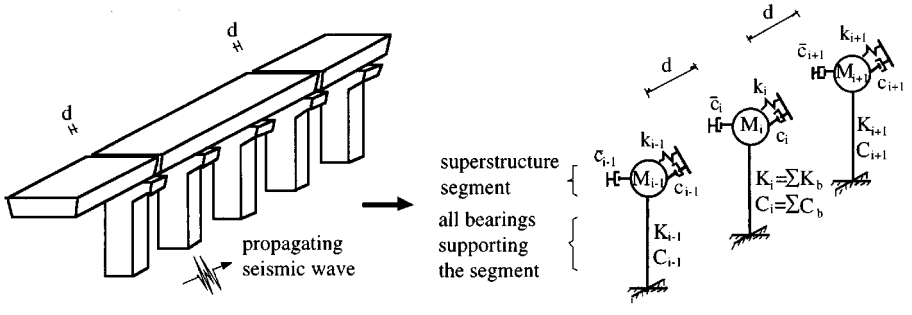

Figure 1. Simplified model of the bridge

Modelling of collisions between superstructure segments

A collision between adjacent superstructure segments is a complicated multi-dimensional process. During impact, the large axial forces in the superstructures, F_L, as well as some transverse friction forces, F_T, due to transverse relative motion of the decks are induced. Since the longitudinal forces F_L are much higher than F_T, it is assumed that during collision there is no sliding in the transverse direction. The assumed mechanism of pounding is illustrated in Figure 2.

The collision in the longitudinal direction is modelled by an impact linear viscoelastic element.[7] The element becomes active when the relative displacement between superstructure segments is smaller than the initial gap d (Figure 1). Thus, the problem of pounding is described by two sets of linear differential equations. The first set is applied when two segments move independently, and the second one when contact between them occurs. Changing from one stage to the other simulates the boundary non-linearity of pounding phenomenon.

The stiffness of the impact element, k_i, is calculated as an axial stiffness of the superstructure segment.[10] The impact element damping, c_i, between two equal masses M_i can be obtained from formula

$$c_i = 2\xi_i \sqrt{k_i \frac{M_i}{2}} \tag{1}$$

where ξ_i is a damping ratio; its value is correlated with a coefficient of restitution, e_i, which describes the energy dissipation during collision incorporating response non-linearities. This relation is given by[7]

$$\xi_i = \frac{-\ln e_i}{\sqrt{\pi^2 + (\ln e_i)^2}} \tag{2}$$

Value of $e_i = 1$ ($\xi_i = 0$) describes fully elastic collision, while value of $e_i = 0$ ($\xi_i = 1$) represents perfectly plastic one. The most common range of coefficient of restitution used to simulate real collision[9] is between 0·5 and 0·75. Based on experimental results, it has been suggested for concrete structures, to use a value of $e_i = 0{\cdot}65$ ($\xi_i = 0{\cdot}14$).[20] It was observed, however that pounding patterns are not really sensitive to the choice of impact element damping.[7]

The dynamic equation of motion in the longitudinal direction of a superstructure segment M_i, including pounding forces due to collisions with adjacent segments, can be written in the form[7]

$$M_i\ddot{x}_i(t) + C_i\dot{x}_i(t) + K_i x_i(t) - F_{i-1,i}(t) + F_{i,i+1}(t) = -M_i\ddot{x}_{gi}(t) \tag{3}$$

where $\ddot{x}_i(t)$, $\dot{x}_i(t)$ and $x_i(t)$ are acceleration, velocity and displacement of the segment relative to the ground, $\ddot{x}_{gi}(t)$ is an acceleration input ground motion; $F_{i-1,i}(t)$ and $F_{i,i+1}(t)$ are impact forces due to pounding of segment M_i with segments M_{i-1} and M_{i+1}, respectively. Their values can be obtained from expressions

$$\begin{aligned}
&F_{i-1,i}(t) = 0 && \text{for } \delta_{i-1,i}(t) \leqslant 0 \quad \text{(no contact)}\\
&F_{i-1,i}(t) = k_{i-1}\delta_{i-1,i}(t) + c_{i-1}\dot{\delta}_{i-1,i}(t) && \text{for } \delta_{i-1,i}(t) > 0 \quad \text{(contact)}\\
&F_{i,i+1}(t) = 0 && \text{for } \delta_{i,i+1}(t) \leqslant 0 \quad \text{(no contact)}\\
&F_{i,i+1}(t) = k_i\delta_{i,i+1}(t) + c_i\dot{\delta}_{i,i+1}(t) && \text{for } \delta_{i,i+1}(t) > 0 \quad \text{(contact)}
\end{aligned} \tag{4}$$

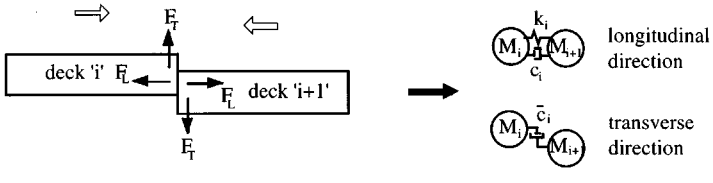

Figure 2. Mechanism of collision between superstructure segments (top view)

where $\delta_{i-1,i}(t)$ and $\delta_{i,i+1}(t)$ are defined in the following way

$$\begin{aligned} \delta_{i-1,i}(t) &= x_{i-1}(t) - x_i(t) - d \\ \delta_{i,i+1}(t) &= x_i(t) - x_{i+1}(t) - d \end{aligned} \tag{5}$$

The interaction of the superstructure segments in the transverse direction is modelled by a linear dashpot element, $\bar{c}_i$, (Figure 2) activated when contact in the longitudinal direction occurs. A high damping value of the dashpot is used in order to simulate the stick condition between segments during collision. A formula for the force in the transverse direction, $\bar{F}_{i,i+1}(t)$, acting between superstructure segments M_i and M_{i+1} can be written as

$$\begin{aligned} &\bar{F}_{i,i+1}(t) = 0 && \text{for } \delta_{i,i+1}(t) \leqslant 0 \quad \text{(no contact)} \\ &\bar{F}_{i,i+1}(t) = \bar{c}_i(\dot{y}_i(t) - \dot{y}_{i+1}(t)) && \text{for } \delta_{i,i+1}(t) > 0 \quad \text{(contact)} \end{aligned} \tag{6}$$

where $\dot{y}_i(t)$ is a velocity of segment M_i in the transverse direction.

By analogy to formula (3), the equation of motion of a single superstructure segment in the transverse direction takes the form

$$M_i\ddot{y}_i(t) + \bar{C}_i\dot{y}_i(t) + \bar{K}_i y_i(t) - \bar{F}_{i-1,i}(t) + \bar{F}_{i,i+1}(t) = -M_i\ddot{y}_{gi}(t) \tag{7}$$

Equation of motion of bridge

Following equations from (3) to (7), the formula describing the dynamic response of the infinite bridge in the longitudinal and transverse directions can be written in a matrix form as

$$\begin{bmatrix} \mathbf{M} & \mathbf{0} \\ \mathbf{0} & \mathbf{M} \end{bmatrix} \begin{bmatrix} \ddot{\mathbf{x}}(t) \\ \ddot{\mathbf{y}}(t) \end{bmatrix} + \begin{bmatrix} \mathbf{C}(t) & \mathbf{0} \\ \mathbf{0} & \bar{\mathbf{C}}(t) \end{bmatrix} \begin{bmatrix} \dot{\mathbf{x}}(t) \\ \dot{\mathbf{y}}(t) \end{bmatrix} + \begin{bmatrix} \mathbf{K}(t) & \mathbf{0} \\ \mathbf{0} & \bar{\mathbf{K}} \end{bmatrix} \begin{bmatrix} \mathbf{x}(t) \\ \mathbf{y}(t) \end{bmatrix} + \begin{bmatrix} \mathbf{D}(t) \\ \mathbf{0} \end{bmatrix} = - \begin{bmatrix} \mathbf{M} & \mathbf{0} \\ \mathbf{0} & \mathbf{M} \end{bmatrix} \begin{bmatrix} \ddot{\mathbf{x}}_g(t) \\ \ddot{\mathbf{y}}_g(t) \end{bmatrix} \tag{8}$$

where $\mathbf{M}$ is a diagonal mass matrix, $\mathbf{x}(t)$, $\mathbf{y}(t)$ are vectors of displacements of segments relative to the ground, $\ddot{\mathbf{x}}_g(t) = [\ \ldots, \ddot{x}_{g,i}(t), \ddot{x}_{g,i+1}(t), \ddot{x}_{g,i+2}(t), \ldots]^T$, $\ddot{\mathbf{y}}_g(t) = [\ \ldots, \ddot{y}_{g,i}(t), \ddot{y}_{g,i+1}(t), \ddot{y}_{g,i+2}(t), \ldots]^T$ are vectors of acceleration ground excitations and

$$\mathbf{C}(t) = \begin{bmatrix} \ddots & & & & \\ & C_i & 0 & 0 & \\ & 0 & C_{i+1} & 0 & \\ & 0 & 0 & C_{i+2} & \\ & & & & \ddots \end{bmatrix}$$

$$+ \begin{bmatrix} \ddots & & & & & \\ & -c_{i-1,i}(t) & c_{i-1,i}(t) + c_{i,i+1}(t) & -c_{i,i+1}(t) & 0 & 0 \\ & 0 & -c_{i,i+1}(t) & c_{i,i+1}(t) + c_{i+1,i+2}(t) & -c_{i+1,i+2}(t) & 0 \\ & 0 & 0 & -c_{i+1,i+2}(t) & c_{i+1,i+2}(t) + c_{i+2,i+3}(t) & -c_{i+2,i+3}(t) \\ & & & & & \ddots \end{bmatrix} \tag{9a}$$

$$\bar{\mathbf{C}}(t)=\begin{bmatrix}\ddots & & & & \\ & C_i & 0 & 0 & \\ & 0 & C_{i+1} & 0 & \\ & 0 & 0 & C_{i+2} & \\ & & & & \ddots\end{bmatrix}$$

$$+\begin{bmatrix}\ddots & & & & & \\ & -\bar{c}_{i-1,i}(t) & \bar{c}_{i-1,i}(t)+\bar{c}_{i,i+1}(t) & -\bar{c}_{i,i+1}(t) & 0 & 0 \\ & 0 & -\bar{c}_{i,i+1}(t) & \bar{c}_{i,i+1}(t)+\bar{c}_{i+1,i+2}(t) & -\bar{c}_{i+1,i+2}(t) & 0 \\ & 0 & 0 & -\bar{c}_{i+1,i+2}(t) & \bar{c}_{i+1,i+2}(t)+\bar{c}_{i+2,i+3}(t) & -\bar{c}_{i+2,i+3}(t) \\ & & & & & \ddots\end{bmatrix} \tag{9b}$$

$$\mathbf{K}(t)=\begin{bmatrix}\ddots & & & & \\ & K_i & 0 & 0 & \\ & 0 & K_{i+1} & 0 & \\ & 0 & 0 & K_{i+2} & \\ & & & & \ddots\end{bmatrix}$$

$$+\begin{bmatrix}\ddots & & & & & \\ & -k_{i-1,i}(t) & k_{i-1,i}(t)+k_{i,i+1}(t) & -k_{i,i+1}(t) & 0 & 0 \\ & 0 & -k_{i,i+1}(t) & k_{i,i+1}(t)+k_{i+1,i+2}(t) & -k_{i+1,i+2}(t) & 0 \\ & 0 & 0 & -k_{i+1,i+2}(t) & k_{i+1,i+2}(t)+k_{i+2,i+3}(t) & -k_{i+2,i+3}(t) \\ & & & & & \ddots\end{bmatrix} \tag{9c}$$

$$\bar{\mathbf{K}}=\begin{bmatrix}\ddots & & & & \\ & K_i & 0 & 0 & \\ & 0 & K_{i+1} & 0 & \\ & 0 & 0 & K_{i+2} & \\ & & & & \ddots\end{bmatrix},\quad \mathbf{D}(t)=\begin{bmatrix}\vdots \\ (k_{i-1,i}(t)-k_{i,i+1}(t))d \\ (k_{i,i+1}(t)-k_{i+1,i+2}(t))d \\ (k_{i+1,i+2}(t)-k_{i+2,i+3}(t))d \\ \vdots\end{bmatrix} \tag{9d}$$

In the matrices of equation (9), elements: $c_{i,i+1}(t)$, $\bar{c}_{i,i+1}(t)$ and $k_{i,i+1}(t)$ apply additional damping and stiffness if contact between segments M_i and M_{i+1} in the longitudinal direction occurs

$$\begin{aligned} c_{i,i+1}(t)=0,\quad k_{i,i+1}(t)=0,\quad \bar{c}_{i,i+1}(t)=0 \quad &\text{for } \delta_{i,i+1}(t)\leqslant 0 \quad \text{(no contact)} \\ c_{i,i+1}(t)=c_i,\quad k_{i,i+1}(t)=k_i,\quad \bar{c}_{i,i+1}(t)=\bar{c}_i \quad &\text{for } \delta_{i,i+1}(t)>0 \quad \text{(contact)} \end{aligned} \tag{10}$$

where $\delta_{i,i+1}(t)$ is given in equation (5).

In the analysis, pounding between superstructure segments is induced due to the seismic wave propagation effect which can be described by identical input ground motion records acting with time lags, τ_i, on supports

along the structure[21]

$$\ddot{x}_{g,i}(t) = \ddot{x}_{g,1}(t - \tau_i), \quad \ddot{y}_{g,i}(t) = \ddot{y}_{g,1}(t - \tau_i) \tag{11}$$

The value of the time lag, τ_i, depends on the apparent seismic wave velocity and the distance between structural supports.

Non-linear model of high-damping rubber bearings

High-Damping Rubber Bearings (HDRBs), due to their energy dissipation properties, are very attractive for the seismic isolation purposes. For design simplicity, they are usually modelled by the equivalent linear formulation.[22] The equivalent stiffness, K_b, and equivalent damping ratio, ξ_b, are computed from the hysteresis loop of the bearing specified for the effective design displacement, x_e, using the following formulae[23]

$$K_b = \frac{F(x_e) - F(-x_e)}{2x_e} \tag{12}$$

$$\xi_b = \frac{\Delta W}{2\pi W} \tag{13}$$

where $F(x_e)$ is a lateral force at displacement x_e, ΔW is energy dissipated in one cycle (area of the loop) and W is the strain energy stored in the bearing

$$W = F(x_e) \cdot x_e \tag{14}$$

However, HDRB shows non-linear behaviour which depends on shear strain level and shear strain rate.[19] It can also be influenced by the axial pressure, loading history and increase of internal temperature. Thus, for more accurate simulation, the strain-rate-dependent model of HDRB is proposed in this paper. In the model, based on the formulation given by Pan and Yang,[24] the horizontal response of the bearing under specified axial load is described by non-linear spring-dashpot element. The shear stiffness and damping coefficients at a given time t are computed from the actual values of displacement and velocity using formulae

$$K_b(x(t), \dot{x}(t)) = a_1 + a_2 x^2(t) + a_3 x^4(t) + \frac{a_4}{\cosh^2(a_5 \dot{x}(t))} + \frac{a_6}{\cosh(a_7 \dot{x}(t))\cosh(a_8 x(t))} \tag{15}$$

$$C_b(x(t), \dot{x}(t)) = \frac{a_9 + a_{10} x^2(t)}{\sqrt{a_{11}^2 + \dot{x}^2(t)}} \tag{16}$$

where a_1–a_{11} are parameters of the model which are obtained by fitting the experimental data using the least-squares optimization method.

PARAMETERS OF ELEVATED HIGHWAY BRIDGE

The model of a base-isolated elevated highway bridge specified according to the 'Manual for Menshin Design of Highway Bridges' is used to study the influence of pounding on structural response.[19] The deck of the bridge is made from three-span-continuous, prestressed concrete segments with a mass of 2×10^4 kg/m. The span length and the width of one superstructure segment are 40 and 14 m, respectively. A substructure consists of reinforced concrete piers of equal height of 11·5 m. Two high-damping rubber bearings support the superstructure at every pier. The cross-sectional area and the height of rubber layers in a single bearing are 0·7921 m^2 and 0·082 m, respectively. The effective stiffness and the equivalent damping ratio for a pair of bearings are given for the design displacement of 0·185 m as $K_b = 2{\cdot}3298 \times 10^7$ N/m and $\xi_b = 0{\cdot}14$. For this value of stiffness, the natural period of the superstructure in both horizontal directions is equal to 1·1643 s. The longitudinal and transverse cross-section of the bridge are presented in Figure 3. Based on the bridge

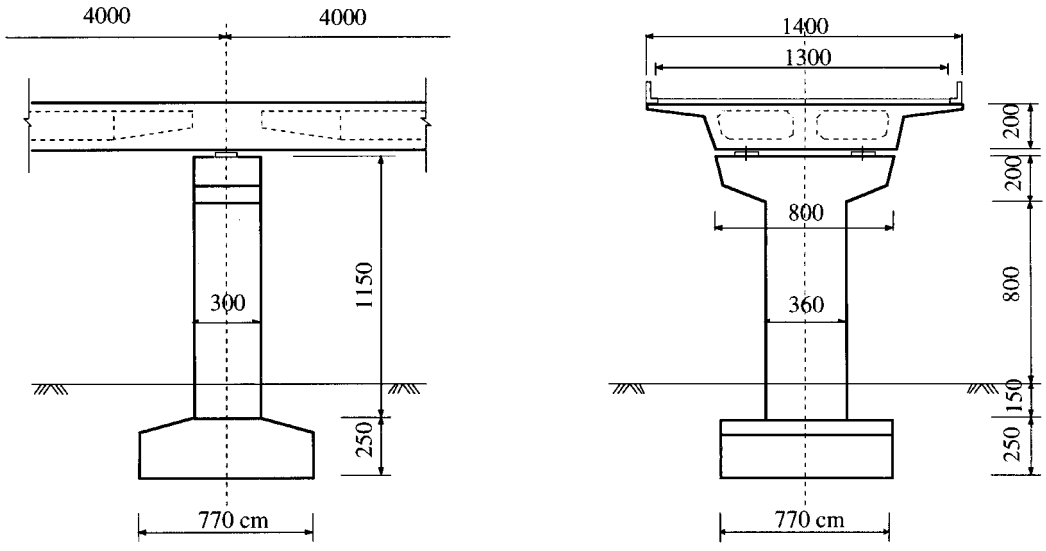

Figure 3. Longitudinal and transverse cross-section of the bridge

properties, the stiffness and damping of the impact elements, used in the structural model, have been calculated as $k_i = 3{\cdot}4751 \times 10^9$ N/m and $c_i = 1{\cdot}8081 \times 10^7$ kg/s, respectively.

Selection of the bridge model

The analysis is focused on the response of a single superstructure segment of an infinitely long bridge. It is easy to understand that the influence of motion of the bridge segments located far from the section of interest decreases with the distance. Since the theoretical derivation of the necessary bridge model and edge conditions is practically impossible, the selection of the model is determined through numerical simulations. The computations are carried out applying the linear model of HDRB, under the longitudinal excitation of NS component of the El Centro earthquake (18 May 1940) scaled to 800 gals. For this ground motion, the response of the single superstructure segment gives the maximum displacement equal to the design displacement of 0·185 m.[19] Some of the results of the numerical simulations conducted on various bridge models for different gap sizes between segments with the apparent seismic wave velocity of 1000 m/s are presented in Figure 4.

By decreasing the number of superstructure segments taken into account, it was found that for models consisting of seven or more segments, the response of the middle segment is very similar. In order to reduce the size of the bridge model even further, and thus significantly speed up the numerical calculations, a five-segment model with simulation of neglected segments by spring-dashpots (with the same properties as impact elements) was studied. It can be seen from Figure 4 that for this configuration, the influence of edge conditions is reduced and the maximum response of the middle segment for different gaps is similar to the case of model with seven segments. Therefore, the simplified five-degree-of-freedom model of the bridge has been chosen for further analysis.

Influence of non-linearity of bearings on bridge response

The non-linear model of HDRB defined by equations (15) and (16) describes the variation of the bearing behaviour with the shear strain and shear strain rate. The dependence of equivalent stiffness and damping

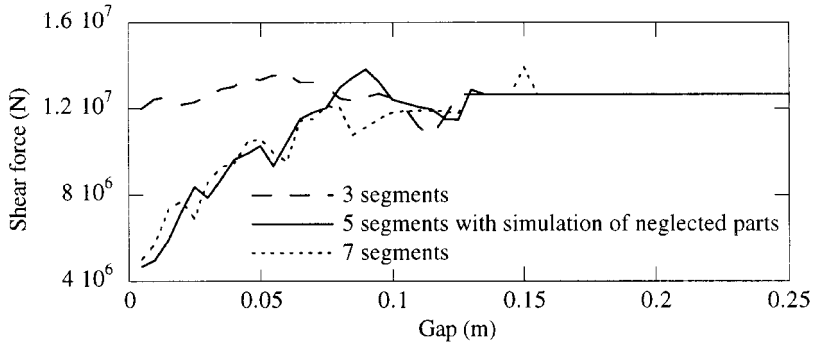

Figure 4. Maximum shear forces of middle segment with respect to gap size for bridge models consisting of different number of segments under El Centro earthquake

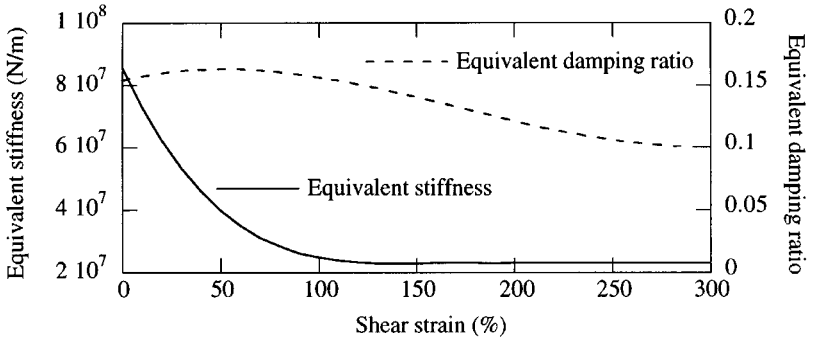

Figure 5. Equivalent stiffness and damping ratio for HDRB with respect to shear strain

ratio on shear strain for the pair of analysed bearings[19] is presented in Figure 5. It can be seen from Figure 5 that the equivalent dynamic parameters of the bearings decrease with the shear strain reaching 300%. The parameters of the non-linear model of HDRB optimized for the given set of data[19] are found to be: $a_1 = 1{\cdot}6074 \times 10^7$, $a_2 = -3{\cdot}7000 \times 10^7$, $a_3 = 8{\cdot}8153 \times 10^8$, $a_4 = 5{\cdot}9956 \times 10^6$, $a_5 = 1{\cdot}5753$, $a_6 = 6{\cdot}0450 \times 10^7$, $a_7 = 7{\cdot}7280$, $a_8 = 48{\cdot}013$, $a_9 = 9{\cdot}7679 \times 10^5$, $a_{10} = 5{\cdot}1964 \times 10^6$, $a_{11} = 0{\cdot}59601$. Comparison of the experimental results and simulated hysteresis loops are shown in Figure 6. It can be seen that the proposed non-linear model can fit well the high stiffness region at low strain level; it can also precisely describe the hardening of the high-damping rubber bearings at bigger displacements.

In order to compare the difference between the linear and non-linear formulations of HDRB, the numerical simulations are conducted on a simplified five-degree-of-freedom bridge model. Figure 7 shows maximum shear forces in the longitudinal direction for the middle segment with respect to the gap size between segments under constant apparent seismic wave velocity of 1000 m/s. It can be observed from this figure that both models give similar results for smaller gap values for which displacements of segments are lower than the design displacement of 0·185 m specified for the linear formulation. However, the maximum shear forces are larger using non-linear model for the range of gap sizes of about 0·09–0·13 m where, due to pounding, displacements are higher than the design value. This is due to the fact that the actual stiffness and damping of HDRB, accurately modelled by the non-linear formulation, decrease with the increase of shear strain (Figure 5), leading to larger displacements and shear forces for superstructure segments. It can be also seen from Figure 7 that the accurate response of the segments can be obtained using a linear model if pounding does not occur.

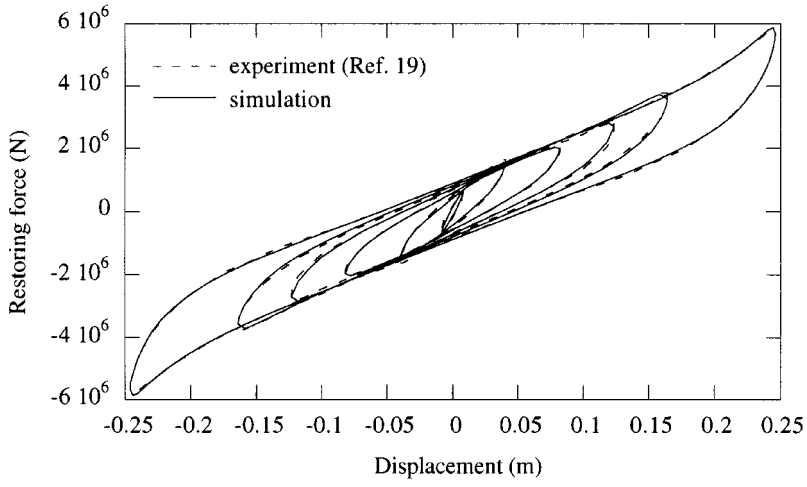

Figure 6. Specified and simulated hysteresis loops for HDRB

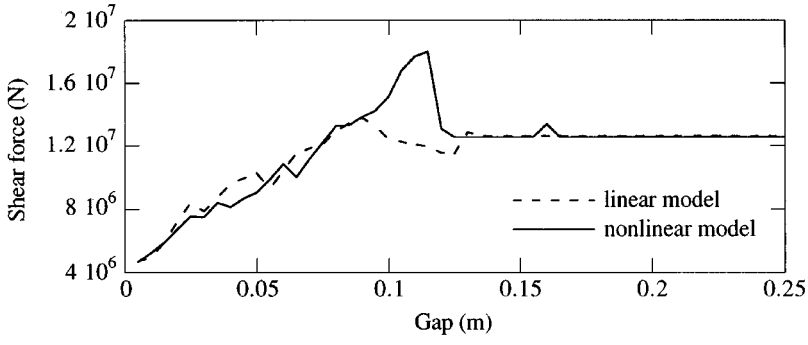

Figure 7. Maximum shear forces with respect to gap size for linear and non-linear models of HDRB under El Centro earthquake

RESPONSE ANALYSIS

The response of five-degree-of-freedom bridge model with the non-linear formulation of HDRB in two horizontal directions is studied under different ground motions. To solve equation of motion (8) numerically, the transition matrix method[25] with constant time step of 0·005 s is used. First, the bridge is subjected to the longitudinal and transverse excitations by NS and EW components of the scaled El Centro earthquake. The apparent seismic wave velocity is set to 1000 m/s. The displacement time histories of the analysed superstructure segment for gap $d = 0{\cdot}01$ m and $d = 0{\cdot}11$ m together with the response when no pounding occurs are presented in Figure 8. For these values of the gap size, the pounding forces defined by equation (4) between the analysed segment and segments from the left and the right side are also shown in Figure 9. The results indicate that pounding patterns can significantly alter the behaviour of the structure. The number of collisions for 0·01 m gap is large; however, the maximum pounding force hardly exceeds 5×10^7 N and the displacement of the superstructure segment is kept within 0·06 m. In this case, most of the hits take place when the segments approach from opposite directions; thus, collisions result in the reduction of displacements. The pounding history for the gap of 0·11 m shows only a few collisions. The first one results in

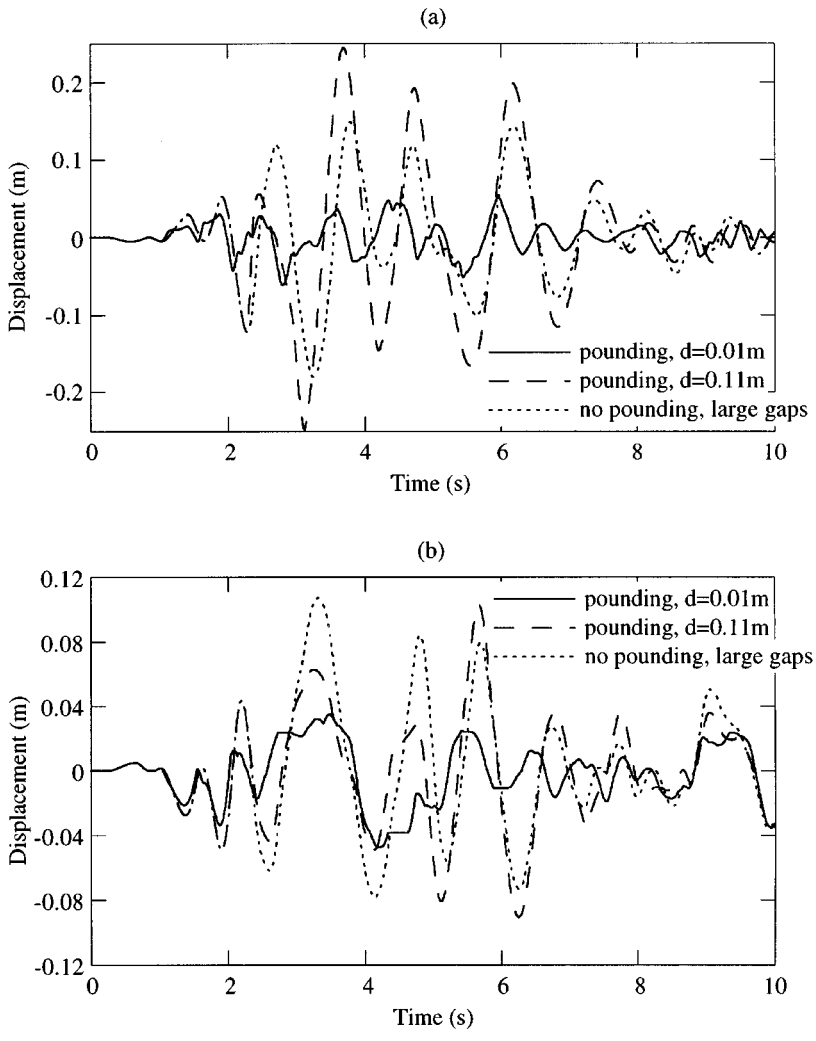

Figure 8. Displacement time histories of segment for different gap sizes under El Centro earthquake for: (a) longitudinal direction; (b) transverse direction

a pounding force of a magnitude twice larger than for the bridge with small gaps. The force of this hit combines with the external excitation and stored elastic energy resulting in very large deformation of the deck. The response of the bridge without pounding is larger than the response with very small gaps and many collisions, while it is smaller than the response with larger gaps for which pounding is still observed.

Analysis with several ground motions is carried out to test the bridge behaviour for different values of the gap between superstructure segments and the apparent seismic wave velocity. Together with the El Centro ground motion, acceleration records of the Kobe (17 January 1995) and Kushiro (15 January 1993) earthquakes (Figures 10 and 11) are also applied. NS components of the ground motions are set to act in the longitudinal direction of the bridge axis and EW components in the transverse one. The records of the events have been scaled to give the response with the maximum shear strain of HDRB not exceeding 300% (Figure 5). Original and scaled peak acceleration values (PGA) of ground motion histories are shown in Table I. The acceleration response spectra for NS components of scaled records are presented in Figure 12.

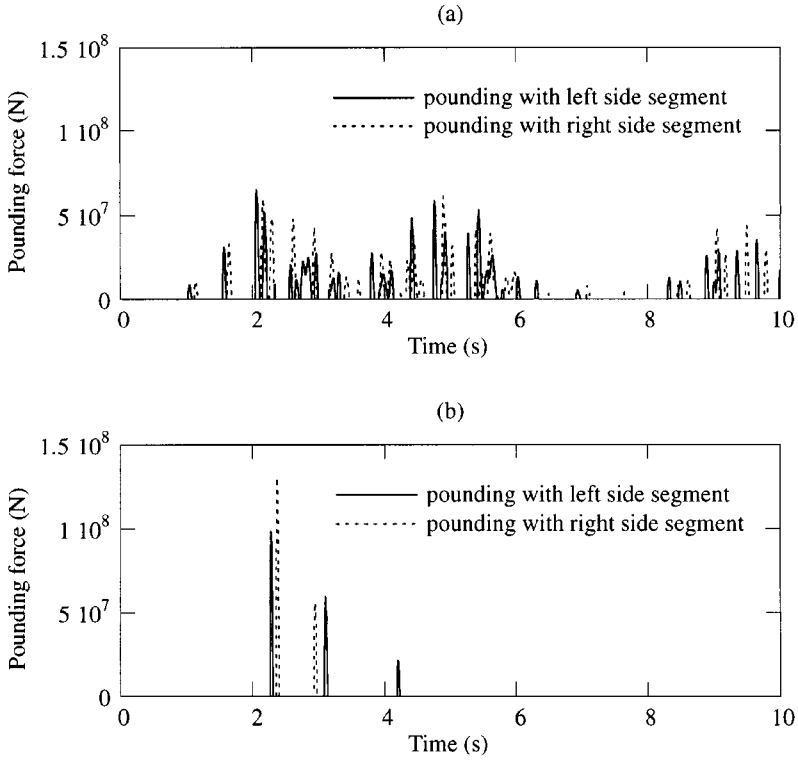

Figure 9. Pounding time histories of analysed segment under El Centro earthquake for: (a) gap $d = 0.01$ m; (b) gap $d = 0.11$ m

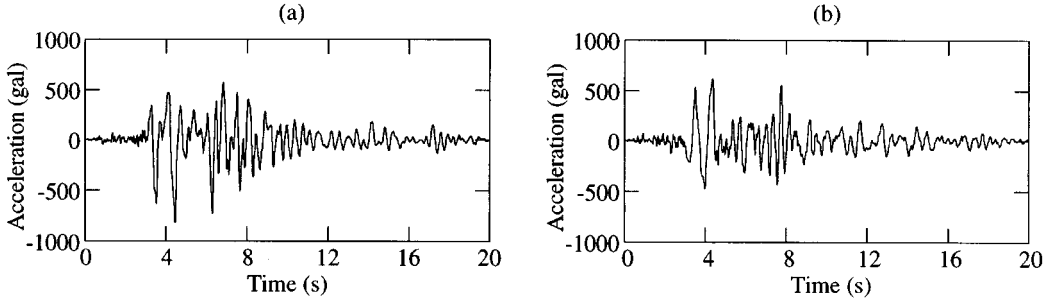

Figure 10. Acceleration records of Kobe earthquake (JMA station): (a) NS component; (b) EW component

Figure 13 shows the maximum shear forces of the middle segment with respect to the gap size and the apparent seismic wave velocity. It can be seen from the graph that the structural response in both directions follows the same patterns for all ground motions used in the analysis. The results show the significant influence of the gap size on the bridge behaviour, especially, in its longitudinal direction. The general tendency indicates that when the gap size becomes bigger, the values of maximum shear forces increase. This trend is maintained until the gap size is large enough to avoid pounding, and then, the maximum shear forces drop to the value corresponding to the unpounding case. Figure 13 also shows the dependence of the apparent seismic wave velocity on the response of the bridge. It can be seen that for smaller values of velocity,

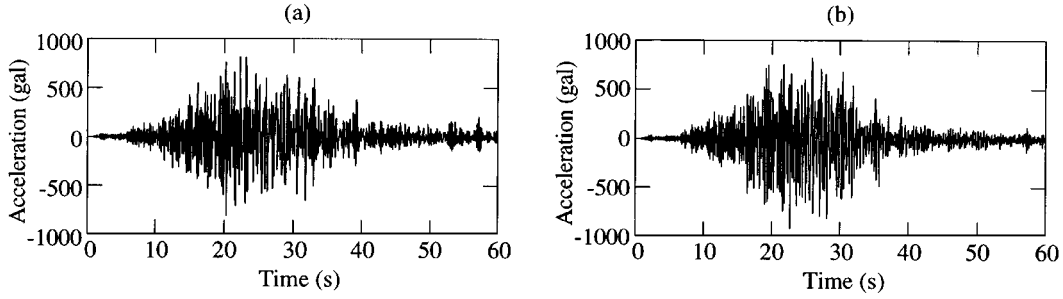

Figure 11. Acceleration records of Kushiro earthquake: (a) NS component; (b) EW component

Table I. Ground motions used in the analysis

Earthquake	Component	Original PGA (gal)	Scale factor	PGA after scaling (gal)
El Centro	NS	340·2	2·3516	800·0
	EW	177·2		416·7
Kobe	NS	817·8	0·6725	550·0
	EW	617·1		415·0
Kushiro	NS	814·7	1·2274	1000·0
	EW	919·1		1128·1

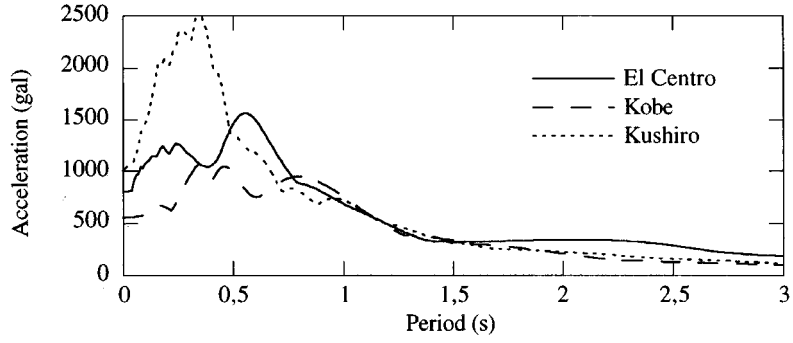

Figure 12. Acceleration response spectra ($\xi = 0{\cdot}14$) for different earthquakes (NS components)

maximum shear forces are lower but a larger gap is needed to prevent pounding. On the other hand, for higher velocities, shear forces are larger, although a smaller gap can be applied to avoid collisions.

A similar tendency in relation to the gap size and the apparent seismic wave velocity is observed for both bridge directions. In the case of the transverse direction, however, different values of these parameters do not modify the behaviour of the structure so significantly.

Figure 14 shows the maximum pounding forces as a function of the gap size for the apparent seismic wave velocity of 1000 m/s. For all events, with the increase of the gap size up to about 0·11–0.13 m, forces due to

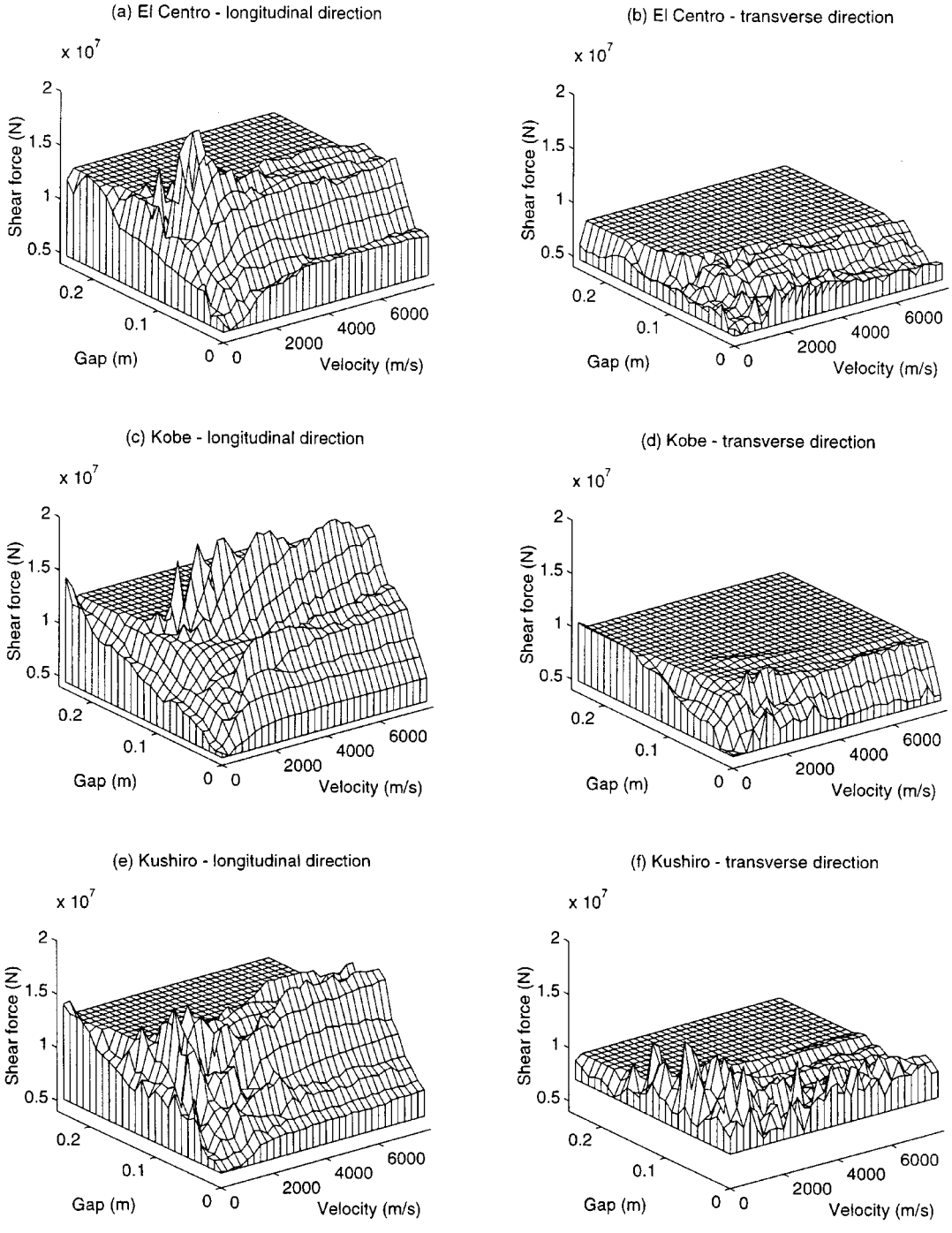

Figure 13. Maximum shear forces with respect to gap size and apparent seismic wave velocity under different earthquakes

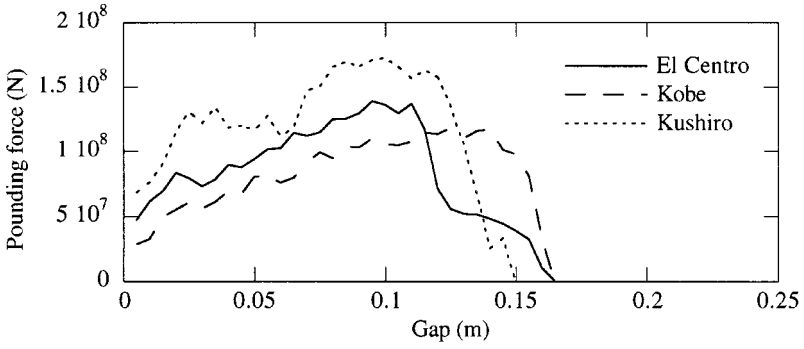

Figure 14. Maximum pounding forces with respect to gap size under different earthquakes

collisions become bigger. Then, their magnitudes fall sharply to zero when gaps are large enough to prevent pounding.

Optimal separation width between superstructure segments

The results of the analysis show the existence of two gap intervals between adjacent superstructure segments for which the smallest structural response in both horizontal directions can be obtained. They indicate that the gap size should be either a very small one or large enough to avoid collisions.

In the case of a large gap size, every superstructure segment vibrates independently and the negative effects of pounding, such as the increase of displacement after collision or damage to deck ends, is prevented. Nevertheless, in order to avoid collisions, a substantial increase of the separation width would be required, especially if the apparent seismic wave velocity is expected to be small. It can be seen from Figure 14 that for the velocity value of 1000 m/s at least 0·17 m would be needed and even that may not be enough for very severe earthquakes, such as Kobe, whose record was scaled down in the analysis. However, enlarging the gaps between adjacent superstructure segments is undesirable since heavy traffic loads moving on the deck are to be carried over the expansion joints.

On the other hand, the interval of a very small gap size is close to the case of nearly fully continuous deck. When the seismic wave travels along the bridge, the long continuous superstructure is subjected to excitations shifted in time in different places. This makes them act in opposite directions at the same time, and thus a smaller response is possible. Expansion joints applied in bridges are designed to accommodate length changes of the superstructure due to thermal, creep and shrinkage effects. They should also allow some space for placement of bridge decks. This usually requires some minimum separation width, which for the analysed bridge should be as big as 0·05 m.[18] However, it can be seen from Figures 14 and 7 that for this value of the gap size, the pounding forces can already be relatively large whereas the reaction forces are only slightly smaller when compared with the unpounding case. Significant reduction of shear and pounding forces can be obtained for gap values of about 0·01 m, although in such a case, the internal forces in the superstructure might occur due to its thermal elongation.

CONCLUSIONS

In this paper, pounding between superstructure segments of an elevated isolated bridge induced by the seismic wave propagation effect has been analysed. The problem has been formulated for longitudinal and transverse motion of the segments. A non-linear model of high-damping rubber bearings has been proposed to enhance the accuracy of pounding prediction.

The results of numerical simulations show that collisions have considerable influence on the structural behaviour, especially, in the longitudinal direction of the bridge. They indicate that the response of the bridge depends much on the gap size between superstructure segments. The largest shear and pounding forces occur for bigger gaps for which collisions are still observed. The results of the analysis also show that the bridge behaviour depends on the apparent seismic wave velocity. Generally speaking, for smaller velocity values the reaction forces are smaller. A similar tendency in relation to the gap size and the apparent seismic wave velocity is observed for both horizontal directions. Although, the response in the transverse direction is not so much influenced by different values of tested parameters.

It has been shown that in order to avoid pounding, a substantial enlargement of the gap sizes between superstructure segments might be required. On the other hand, the reaction forces can be reduced by allowing pounding, if very small gaps between segments are applied. Although the pounding forces in this case are relatively low, the internal forces may occur in the superstructure, due to its thermal elongation, if the size of the gaps is too small.

The study presented in the paper assumes a simple collision mechanism and simplifies the dynamics of a superstructure segment to single-degree-of-freedom system. Thus, the obtained results provide the qualitative information. Further research including a more complete collision modelling and incorporating complex response of piers, such as non-linear response under large loading and interaction between pier foundation and soil, should be conducted.

REFERENCES

1. S. S. Tezcan, V. Yerlici and H. T. Durgunoglu, 'A reconnaissance report for the Romanian earthquake of 4 March 1977', *Earthquake Engng. Struct. Dyn.* **6**, 397–421 (1978).
2. E. Rosenblueth and R. Meli, 'The 1985 earthquake: causes and effects in Mexico City', *Concrete Int.* **8**(5), 23–34 (1986).
3. K. Kasai and B. F. Maison, 'Structural pounding', *Reflections on the Loma Prieta Earthquake of October 17, 1989*, Chapter 6, Structural Engineers Association of California (SEAOC), 1991.
4. M. J. N. Priestley, F. Seible and G. M. Calvi, *Seismic Design and Retrofit of Bridges*, Wiley, New York, 1996.
5. P. K. Malhotra, M. J. Huang and A. F. Shakal, 'Seismic interaction at separation joints of an instrumented concrete bridge', *Earthquake Engng. Struct. Dyn.* **24**, 1055–1067 (1995).
6. H. Otsuka, S. Unjoh, T. Terayama, J. Hoshikuma and K. Kosa, 'Damage to highway bridges by the 1995 Hyogoken Nanbu earthquake and the retrofit of highway bridges in Japan', *3rd U.S.–Japan Workshop on Seismic Retrofit of Bridges*, Osaka, Japan, 10–11 December 1996.
7. S. A. Anagnostopoulos, 'Pounding of buildings in series during earthquakes', *Earthquake Engng. Struct. Dyn.* **16**, 443–456 (1988).
8. M. Papadrakakis, H. Mouzakis, N. Plevris and S. Bitzarakis, 'A Lagrange multiplier solution method for pounding of buildings during earthquakes', *Earthquake Engng. Struct. Dyn.* **20**, 981–998 (1991).
9. S. A. Anagnostopoulos and K. V. Spiliopoulos, 'An investigation of earthquake induced pounding between adjacent buildings', *Earthquake Engng. Struct. Dyn.* **21**, 289–302 (1992).
10. B. F. Maison and K. Kasai, 'Dynamics of pounding when two buildings collide', *Earthquake Engng. Struct. Dyn.* **21**, 771–786 (1992).
11. M. Papadrakakis, C. Apostolopoulou, A. Zacharopoulos and S. Bitzarakis, 'Three-dimensional simulation of structural pounding during earthquakes', *J. Engng. Mech.* **122**(5), 423–431 (1996).
12. K. Kasai, A. R. Jagiasi and V. Jeng, 'Inelastic vibration phase theory for seismic pounding mitigation', *J. Struct. Engng.* **122**(10), 1136–1159 (1996).
13. B. D. Westermo, 'The dynamics of interstructural connection to prevent pounding', *Earthquake Engng. Struct. Dyn.* **18**, 687–699 (1989).
14. T. Kobori, T. Yamada, Y. Takenaka, Y. Maeda and I. Nishimura, 'Effect of dynamic tuned connector on reduction of seismic response — application to adjacent office buildings —', *Proc. 9th World Conf. Earthquake Engineering*, Vol. V, Tokyo, Kyoto, 2–9 August 1988, pp. 773–778.
15. S. A. Anagnostopoulos, 'Building pounding re-examined: how serious a problem is it?', *11th World Conf. Earthquake Engineering*, Acapulco, Mexico, 23–28 June 1996, paper No. 2108.
16. X. Ma and C. P. Pantelides, 'Nonlinear pounding of bridges in earthquakes', *Structures Congress ASCE*, Chicago, 17–19 April 1996, pp. 1180–1187.
17. K. Kawashima and M. Yabe, 'Effectiveness of unseating prevention device with energy dissipation', *4th U.S.–Japan Workshop on Earthquake Protective Systems for Bridges*, Osaka, Japan, 10–11 December 1996.
18. Japanese Road Association, *Highway Design Specifications*, Tokyo, 1996 (in Japanese).
19. K. Kawashima, M. Okado and M. Horikawa, 'Design example of a highway bridge based on the Manual for Menshin Design of Highway Bridges', *Recent Selected Publications at Earthquake Engineering Division, Public Works Research Institute*, No. 2, Ministry of Construction, Tsukuba, Japan, May, 1993, pp. 191–208.
20. J. Azevedo and R. Bento, 'Design criteria for buildings subjected to pounding', *11th World Conf. Earthquake Engineering*, Acapulco, Mexico, 23–28 June 1996, paper No. 1063.

21. V. Jeng and K. Kasai, 'Spectral relative motion of two structures due to seismic travel waves', *J. Struct. Engng.* **122(**10), 1128–1135 (1996).
22. E. Mele, A. De Luca and R. Ramasco, 'The effect of using different device numerical models on the global nonlinear behaviour of base isolated structures', *11th World Conf. Earthquake Engineering*, Acapulco, Mexico, 23–28 June 1996, paper No. 1541.
23. H. Sugita and S. A. Mahin, 'Manual for Menshin Design of Highway Bridges: Ministry of Construction, Japan', *EERC Report No. 94/10*, Earthquake Engineering Research Center, University of California at Berkeley, CA, 1994.
24. T. C. Pan and G. Yang, 'Nonlinear analysis of base-isolated MDOF structures', *11th World Conf. Earthquake Engineering*, Acapulco, Mexico, 23–28 June 1996, paper No. 1534.
25. L. Meirovitch, *Dynamics and Control of Structures*, Wiley, New York, 1990.

